Progress towards hydro-equivalent ignition in OMEGA direct-drive DT-layered implosions

L. Ceurvorst,[1, a)] R. Betti,[1] V. Gopalaswamy,[1] A. Lees,[1] J. P. Knauer,[1] M. J. Rosenberg,[1] D. Patel,[1] R. Ejaz,[1] C. A. Williams,[1] K. M. Woo,[1] P. S. Farmakis,[1] D. Cao,[1] C. A. Thomas,[1] I. V. Igumenshchev,[1] K. S. Anderson,[1] T. J. B. Collins,[1] R. Epstein,[1] A. A. Solodov,[1] C. J. Forrest,[1] C. Stoeckl,[1] R. C. Shah,[1] V. Yu. Glebov,[1] H. McClow,[1] V. N. Goncharov,[1] R. K. Follett,[1] D. Turnbull,[1] K. Churnetski,[1] D. H. Froula,[1] S. P. Regan,[1] R. T. Janezic,[1] C. Fella,[1] M. W. Koch,[1] W. T. Shmayda,[1] M. J. Bonino,[1] D. R. Harding,[1] S. Sampat,[1] K. A. Bauer,[1] S. F. B. Morse,[1] M. Gatu Johnson,[2] C. Wink,[2] R. D. Petrasso,[2] C. K. Li,[2] J. A. Fenje,[2] C. Shuldberg,[3] J. Murray,[3] D. Guzman,[3] B. Serrato,[3] and M. Farrell[3]

[1)] *Laboratory for Laser Energetics, University of Rochester, Rochester, NY 14623-1299, USA*

[2)] *Massachusetts Institute of Technology, Cambridge, MA 02139, USA*

[3)] *General Atomics, San Diego, California 92121*

(Dated: 2 December 2024)

Considerable progress has been made in DT-layered implosion experiments on the OMEGA Laser System, bringing the possibility of thermonuclear ignition in direct-drive configurations with megajoule-class lasers closer to reality. Doing so has required navigating the balance between improved 1D performance and multidimensional stability. Using statistical modeling based on over 350 cryogenic implosions to identify various degradation mechanisms, and combined with multidimensional simulations and experimental techniques such as target offsets to combat residual flows, core conditions have repeatably been achieved that extrapolate to the burning-plasma state when scaled to 2.15 MJ of symmetric laser illumination. Using high implosion velocities ($> 450\,\mathrm{km/s}$) and moderately high adiabats (~ 5), these experiments produced record-high scaled Lawson parameters in direct drive equal to $89 \pm 2\%$ of that required for ignition with expected yields of up to $1.5 \pm 0.2\,\mathrm{MJ}$. To improve these results still further, focused-physics studies are performed to improve physics understanding and identify routes to even greater performance. Recent studies include investigations into the impact of mounting features, laser imprint, reduced fuel temperatures, and greater on-target intensities through subscale experiments. This manuscript gives a summary of the cryogenic direct-drive program on the OMEGA laser, including routes taken to achieve the current best performance, the status of recent focused-physics investigations, and future designs—such as target solutions to laser imprint and reducing vapor density to increase convergence—that are expected to soon produce hydro-equivalent ignition on OMEGA.

I. INTRODUCTION

Inertial confinement fusion (ICF)[1–3] compresses and heats fuel composed of deuterium (D) and tritium (T) to extreme levels, allowing collisions between the fuel ions to have enough kinetic energy to quantum tunnel through their Coulomb barrier and fuse to produce a 14.1-MeV neutron and a 3.5-MeV α particle. To make the fusion of these particles energy efficient, α particles must collide with the fuel and deposit their energy.[4–6] If this is done so that the heating of the fuel exceeds its energy losses, the target is said to have ignited, leading to runaway energy production in the fuel.

Laser ICF achieves this by cryogenically freezing a layer of DT fuel within a low-Z shell and ablating the surface of the capsule with incident radiation. The ablation pressure accelerates the shell inward at high velocities (300 to 600 km/s). The central pressure within the capsule increases as the shell is driven inward, slowing the imploding capsule. Upon reaching stagnation, the kinetic energy of the shell is converted into internal energy, producing central temperatures in the low-density (30 to $100\,\mathrm{g/cm^3}$) hot spot of several kiloelectronvolts. Fusion occurs, and the resulting α particles travel through the dense fuel shell. When the shell's areal density (ρR) is great enough, α particles collide with its fuel, depositing their energy and amplifying the fusion reaction rates—a process known as α heating. As performance improves, α heating will become the dominant source of input energy to the system, a state known as the burning-plasma regime. At this point, yield amplification from the α particles rapidly increases absolute yields, making this an important milestone as implosions progress toward ignition. For the system to ignite, it is estimated that the product of the hot spot's temperature and areal density of the fuel must exceed $5\,\mathrm{keV} \times 0.3\,\mathrm{g/cm^2}$.[2,7–9]

Within laser-based ICF, there are two major approaches to irradiating the capsule and producing these implosions. The first, indirect drive,[5,7,10] mounts its capsules within a high-Z cylinder known as a hohlraum. Laser beams are focused onto the interior surface of the hohlraum, converting laser energy to x rays that fill the chamber's cavity, producing a radiation bath that ablates material off of the capsule surface. While this produces smooth irradiation of the target, it comes at the

[a)] lceurvorst@lle.rochester.edu

cost of efficiency. The conversion to x-ray energy, the filling of the hohlraum, and energy losses through the laser entrance holes significantly lowers the coupling of laser energy to the fusion capsule.[11] Direct-drive ICF seeks to reclaim this efficiency by foregoing the hohlraum and directly illuminating the target surface with laser beams, resulting in about five times more energy coupling to the target. However, this approach faces its own set of challenges.[12] By using coherent laser light rather than incoherent x rays,[13] implosions become more sensitive to low- and mid-mode perturbations seeded by beam pointing and the tiling pattern of multiple beams,[14,15] as well as high-mode modulations from speckling patterns in single-beam spatial profiles.[16–18] Indirect- versus direct-drive ICF is then a trade-off between stability and efficiency. However, they both rely on the same underlying physics, and the recent ignition results in indirect drive[19–21] at the National Ignition Facility (NIF)[22] have confirmed the physics of ignition and propagating burn underpinning all ICF research. As this research now turns from achieving ignition to maximizing gain—the energy produced by fusion reactions divided by the input laser energy—it is crucial to investigate paths such as direct drive to improve energy coupling and lower the required input laser energy.

This manuscript provides a summary of the cryogenic direct-drive ICF program performed on the OMEGA laser[23] at the University of Rochester's Laboratory for Laser Energetics, where implosions have now repeatably reached the scaled burning-plasma state.[24] Sec. II A introduces metrics used to evaluate the performance of implosions in ICF and how to scale these metrics between different laser energies.[25,26] Sec. II B then presents a framework to interpret implosion results through statistical modeling to explain the primary limiters of performance. A brief overview of how the scaled burning-plasma state was reached is provided in Sec. III, describing the implosion design adjustments made to maximize performance in integrated cryogenic implosions. Recent focused-physics studies are then presented in Sec. IV, where research is now centered on maximizing the convergence of implosions to improve areal densities through single-variable studies. Many of these platforms are ongoing, and future research plans to enhance convergence and areal densities are discussed in Sec. V alongside other near- to mid-term research avenues. Finally, Sec. VI provides a summary of these results, progress, and future directions.

II. METRICS AND STATISTICAL MODELING

A. Performance metrics and hydrodynamic scaling

To understand the quality of implosions, it is important to derive metrics that can be applied to a variety of laser energies. One such metric is the normalized Lawson parameter χ.[6,27] This is given by

$$\chi = \frac{P\tau}{[P\tau]_{\rm ign}} \sim \left[(\rho R)^2 \left(\frac{Y_{\rm DT}}{M_{\rm DT}}\right)\right]^{1/3}, \tag{1}$$

where P is the hot-spot pressure, τ is the confinement time, and the system is normalized to the levels required for ignition $[P\tau]_{\rm ign}$, where the self-heating of the hot spot exceeds its energy losses.[2] The Lawson parameter required for ignition goes as $[P\tau]_{\rm ign} = 24/\varepsilon_\alpha S(T_0)$ where ε_α is the alpha-particle birth energy and $S(T_0)$ is a function of the central hot-spot temperature T_0. This function reaches a maximum at $T_0 \simeq 19\,\text{keV}$, though $T_0 \sim 5\,\text{keV}$ is more common in ICF.[28] The principles of the Lawson parameter apply to both direct- and indirect-drive implosions and have been validated through the recent achievement of ignition on the NIF.[19–21] As shown on the right side of this equation, this parameter can be rewritten as a function of the experimentally inferred parameters of areal density ρR, DT yield $Y_{\rm DT}$, and stagnated mass $M_{\rm DT}$.[28–30] To reach ignition, it is necessary to produce implosions with $\chi > 1$.

The OMEGA Laser System, however, does not have the energy required to produce the conditions required for ignition. While the NIF can produce drive energies of 2.15 MJ with plans to increase this still further in the near term, OMEGA is limited to slightly under 30 kJ. This necessarily results in fusion hot-spot radii $R_{\rm hs}$ much smaller than the alpha-particle mean free path λ_α. It is therefore necessary to project the performance of implosions on OMEGA to larger scales to understand what is achievable on an ignition-scale facility. This is accomplished through hydrodynamic scaling.[26,31,32] Various quantities such as the fuel entropy, implosion velocity, and hot-spot pressures are maintained in this scaling so that the increase in alpha heating comes solely from the size increase, $R_{\rm hs} > \lambda_\alpha$. In this scaling, confinement time goes as $\tau \sim R_{\rm hs}$. This means that $\chi \sim P\tau \propto R_{\rm hs}$. The hot-spot energy goes as $E_{\rm hs} \propto R_{\rm hs}^3 P_{\rm hs}$. Noting that $P_{\rm hs}$ is constant across scales and assuming similar energy coupling from the laser to the hot spot, $E_{\rm L} \propto E_{\rm hs} \propto R_{\rm hs}^3$. This latter assumption requires additional verification, though some experiments to directly assess hydroscaling have shown reasonable agreement.[4,24–26] Combining these equations gives:

$$\chi_{\rm MJ} \approx \chi_{\rm OMEGA} \left(\frac{E_{\rm L}^{\rm MJ}}{E_{\rm L}^{\rm OMEGA}}\right)^{1/3}, \tag{2}$$

where $E_{\rm L}^{\rm OMEGA}$ and $\chi_{\rm OMEGA}$ are the energy and χ of OMEGA implosions, respectively, and $E_{\rm L}^{\rm MJ}$ and $\chi_{\rm MJ}$ are the energy and projected χ to a MJ-class facility. In this paper, $E_{\rm L}^{\rm MJ} = 2.15\,\text{MJ}$ is chosen to match the current drive energy of the NIF. Refinements have been made to Eq. 2 to account for higher-order effects, but its basic working principles have been validated through both numerical[30,31,33] and experimental[26,34,35] studies. To enable studies at a range of drive energies and spatial scales

on OMEGA, χ_{MJ} is the standard metric used to measure the quality of implosions on OMEGA.

It should be noted that in addition to the scaled ignition state achieved when $\chi_{\mathrm{MJ}} > 1$, a second region of interest lies in $\chi_{\mathrm{MJ}} > 0.8$. This is the scaled burning-plasma state where, at full scale, α-particle heating would become the dominant source of energy input into the implosions.[6,10] As stated in Sec. I, this leads to a significant steepening of the slope of scaled yields and allows projected gain to exceed unity around $\chi_{\mathrm{MJ}} \approx 0.92$ in direct drive, occurring prior to ignition due to the efficiency of the laser-to-target energy coupling. As will be shown in Sec. III, implosions on OMEGA are now able to consistently reach the scaled burning-plasma state and are nearing projected unity gain.[24]

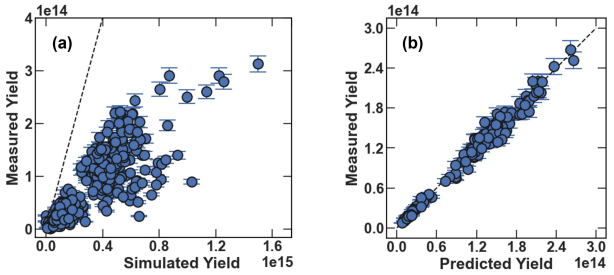

FIG. 1. Statistical modeling of OMEGA implosions. (a) The experimental yield consistently falls below LILAC-predicted yields due to multidimensional effects. (b) When the simulated yields are adjusted with statistical modeling, both the accuracy and precision of these predictions are significantly improved.

B. Statistical modeling

A great deal of work is focused on developing state-of-the-art, multidimensional models such as DRACO in 2D[14] and ASTER-IFRIIT in 3D.[15,36,37] Research with these models is crucial to understanding the physics of, for instance, the evolution of target defects,[38] or the effects of beam polarization on cross-beam energy transfer (CBET) and hot spot morphology.[39,40] Machine-learning models have been developed to provide 3D hot-spot reconstructions to better inform decisions between implosions during an experimental campaign.[41,42] These studies have played a large role in the direction of OMEGA's cryo program, and as new models are developed, this role is expected to continue increasing. However, for simplicity of communication, this manuscript will focus on a technique known as statistical modeling.[25,43] This technique provides a framework to understand the dependencies of cryogenic implosions on OMEGA,[44] and it is possible only because of the large (over 350 at the time of writing) number of implosions performed at this facility.

The statistical model (SM) is a nonlinear piecewise regression applied to the database of OMEGA cryogenic implosions to predict the yield-over-clean (YOC)—that is, the experimental yield divided by the 1D-predicted yield. This enables accurate yield predictions using 1D LILAC simulations, accounting for multidimensional effects through statistics rather than 2D and 3D modeling.[44] As shown in Fig. 1, the statistical model accurately predicts the YOC of implosions with 8% variance around the experimentally measured YOC. This is accurate across a wide range of adiabats (2.5 to 6.0), convergence ratios (10 to 25), implosion velocities (250 km/s to 600 km/s), and drive intensities (0.4×10^{14} W/cm^2 to 1.6×10^{15} W/cm^2). However, understanding the performance of multidimensional parameters such as areal density is currently only possible through higher-dimensional simulations and continues to be a subject of ongoing research.[15] Nonetheless, the success in predicting scalar parameters such as YOC makes statistical modeling a powerful tool for implosion design and a useful framework for interpreting experimental results. While the statistical model's values presented here are specific for OMEGA implosions, this technique and the identified yield dependencies are expected to be extendable to future spherical-direct-drive facilities.

Beyond accurately predicting the YOC of implosion designs, the statistical model can be used to gain insights into the underlying degradation mechanisms of these implosions by analyzing each of the YOC's dependencies. The current fitted equation of the YOC is given by

$$\mathrm{YOC_{SM}} \sim \hat{S}^{0.4-0.85}\hat{C}^{-0.7}\hat{R}^{2.3-4.2}\hat{T}^{-1.4}\hat{H}^{1.2}. \quad (3)$$

Note that some of the exponents represent a range due to the piecewise nature of the statistical model.[25] These five terms are given, and their roles in degrading implosion performance, are described as follows.[44]

$\hat{S} = (\alpha_F/3)^{1.1}/(\mathrm{IFAR}/20)$ is the stability factor, where α_F is the minimum adiabat and IFAR is the in-flight aspect ratio. It is derived both experimentally[45] and from the nonlinear Rayleigh–Taylor growth rates that amplify surface modulations,[46] providing a metric of how robust an implosion is to short-wavelength perturbations such as those from laser imprint and target defects.[47] Targets with higher IFARs have thinner shells in flight, making them more susceptible to perforation. Lower adiabats improve the compressibility of the shells, lowering the ablation velocity, $v_a \propto \alpha_F^{0.6}$,[31] and reducing its stabilizing effects on high-frequency perturbations amplified by the Rayleigh–Taylor instability. As a result, implosions with low stability factors are more susceptible to perforation by short-wavelength modulations, reducing their confinement and overall performance. The piecewise nature of this parameter can be understood as follows. The most unstable implosions have heuristically been found to occur at $\hat{S} < 0.8$. In this regime, short-wavelength perturbations grow large enough to reach the inner surface of the ice layer, destroying confinement and resulting in degradation factors of $\hat{S}^{0.85}$. Above this value, the perturbations are confined within the ice

layer, weakening the piston action, but still confining the hot spot, causing the YOC to go as $\hat{S}^{0.4}$. Finally, extremely stable implosions with $\hat{S} > 2.3$ either have low enough IFARs or high enough adiabats that the effects of these short-wavelength perturbations have been almost entirely negated, resulting in no degradation from this factor.

$\hat{C} = R_{\rm t}/R_{\rm HS}$ is the convergence ratio, where $R_{\rm t}$ is the initial target radius and $R_{\rm HS}$ is the final hot-spot radius. The more a capsule converges, the greater its sensitivity to low- and mid-mode perturbations.[43]

$\hat{R} = R_{\rm b}/R_{\rm t}$ is related to the beam overlap on target, where $R_{\rm b}$ is the focused–drive beam radius. The phase plates on OMEGA were designed to provide quasi-uniform illumination on an 860-μm-diam target. Due to beam tiling, though, some level of mode-10 perturbations are inevitable.[40] As this ratio is varied away from 0.87, where the hard-sphere beam-mode pattern is minimized,[43] the amplitude of those perturbations increases, resulting in a non-spherical hot spot. For $\hat{R} > 0.87$, the degradation from beam overlap goes as $\hat{R}^{2.3}$. As $\hat{R}$ decreases below its ideal, fewer beams overlap on the target, increasing the target's sensitivity to random variations in the power of individual beams (power balance) and laser imprint. The beam-mode tiling pattern on the target rapidly worsens in this regime as well, further degrading performance as $\hat{R}^{4.2}$.[43]

$\hat{T} = T_{\rm max}/T_{\rm min}$ is the apparent temperature asymmetry, where $T_{\rm max}$ and $T_{\rm min}$ are, respectively, the maximum and minimum apparent ion temperatures observed with the neutron time-of-flight (nTOF) detectors. This is the only parameter in the statistical model that is not predicted. Rather, it is a posterior correction to infer the detrimental effects of the unintended flow velocity—the bulk motion of the hot spot at stagnation. Detectors along the axis of the flow will see a broadened DT energy peak, giving a greater inferred ion temperature, while detectors perpendicular to it will not see any broadening.[48,49] Because of this, the ratio of the maximum and minimum observed temperatures is a robust measurement of mode-1 asymmetries and flows when it exceeds the statistical variation level, $\hat{T} \geq 1.14$. Below this level, this correction is ignored as effects from flow velocities become masked by measurement uncertainties in the detectors. Ideal implosions have no flow velocities on stagnation to maximize the conversion of kinetic to internal energy. Any flows represent residual kinetic energy, reducing the overall performance of the implosion.[50]

$\hat{H}$ is the YOC predicted by 1D LILAC simulations when ^{3}He is introduced into the capsule vapor. ^{3}He results from tritium decay, so the longer the time between when the capsules are filled and when they are imploded, the more ^{3}He will exist in the vapor. It has been observed that longer fill times result in more degradation of yield than predicted by LILAC. It remains unclear if this is due solely to the ^{3}He concentration or if beta decay causes detrimental damage to the ablator.

To summarize, the statistical model predicts that maximum yield-over-clean is achieved by designing implosions with large stability factors (high adiabats and low IFARs), low convergence, targets with outer diameters near 860 μm, low flows, and short fill-to-shot times. However, in 1D, the best-performing implosions have high implosion velocities, low adiabats, high convergence, and high IFARs.[24] Overall performance is estimated by multiplying the 1D-predicted yield by the staistical-model–predicted YOC. Therefore, progress is made by balancing these various degradation mechanisms against 1D performance. Navigating this balance to maximize performance is the primary goal of the cryogenic Optimization Campaign.

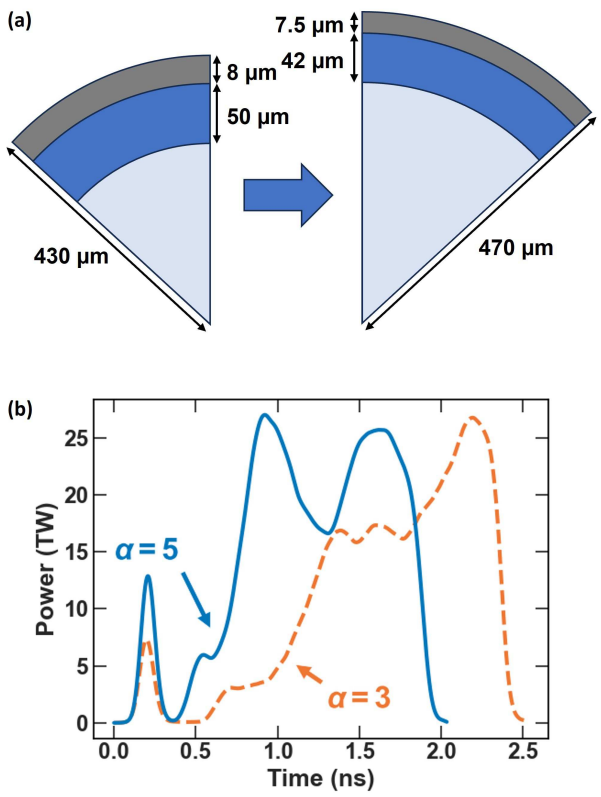

FIG. 2. Statistical model optimizations made to implosion designs. Shown are (a) pie diagrams of typical target designs both before (left) and after (right) these changes were implemented, and (b) typical pulse shapes before (orange dashed) and after (solid blue) the optimization.

III. THE OPTIMIZATION CAMPAIGN

Using the statistical model's framework alongside multidimensional numerical investigations, several adjustments have been made to implosion designs as part of the Optimization Campaign.[24] To begin, the fill cycle—the time from when a capsule is filled with fuel and when it is shot—was reduced from ten days to three days, improving the $\hat{H}$ term in Eq. 3. Further, as shown in Fig. 2(a),

the diameter of the targets increased from 860 µm to ∼940 µm. This decreases the beam mode $\hat{R}$, which is shown in Eq. 3 to reduce overall stability due to mid-mode asymmetries. However, it also reduces the beam overlap on target, reducing CBET to increase energy coupling and improve 1D performance. The targets also feature thinner ice layers and ablators. This increases the implosion velocity, further increasing 1D-predicted yields. On the other hand, the combination of larger diameters and thinner shells increases the IFARs, thereby lowering the stability factor $\hat{S}$, making these implosions more susceptible to high-mode asymmetries such as laser imprint.

To counteract the increased IFARs, the temporal profiles of the laser pulses have been optimized as well [Fig. 2(b)]. The picket and foot of the laser pulses have increased in power to raise the adiabat of the implosions. Additionally, a double-spike pulse shape is now used, where the main drive reaches maximum power at the beginning and end of the pulse with a reduction in power in the center. This maximizes the energy coupled at the start of the drive, when the shell radius is still large and conduction zones are relatively small, and maximum compression to be realized at the end of the pulse. By lowering the power in the center, the shell moderately decompresses in flight, lowering the IFAR. This is also expected to reduce hot-electron preheat since hot electrons are only produced during the second spike, though this effect is not captured by statistical modeling. Combined with the increased adiabat set by the picket and foot, this restores the stability factor to provide robust implosions. Additionally, because the implosion velocities are faster, the pulse length is shortened to ∼1.9 ns. This increases the average power, further increasing energy coupling and implosion velocities.

Other experimental techniques have been used to improve implosion performance. Prior to performing cryogenic implosions, the laser beams are pointed to target chamber center (TCC), and low-mode asymmetries are drastically reduced using precision repointing techniques.[52] Nonetheless, residual kinetic energy in the hot spot (i.e., mode-1 asymmetry) is still observed in implosions. To address the degradation caused by these flows—$\hat{T}$ in Eq. 3—targets are now offset from TCC. The distance and direction of this offset are determined by the nTOF-inferred flow velocities during an experiment.[49] This slightly adjusts the laser intensity profile on the target surface and has been shown to significantly improve flow velocities, symmetry, and overall performance.

Finally, the ablator is now doped with silicon in its outermost layer. This has been shown both numerically and experimentally to boost the absorption of laser energy while suppressing parametric phenomena such as the two-plasmon–decay instability. These instabilities would otherwise generate hot electrons that preheat the target, increasing the target's adiabat beyond its design specification and limiting implosion performance.

These techniques have significantly improved both the hydroscaled Lawson parameters and fusion yields of cryogenic implosions on OMEGA. Figure 3 shows these metrics extrapolated to 2.15 MJ of driver energy for all performance-focused cryogenic implosions. Applying the target and laser pulse improvements guided by the statistical model more than doubled the extrapolated fusion yield at similar extrapolated Lawson parameters by improving the 3D symmetry and robustness of implosions. Ongoing optimizations brought these implosions closer to the scaled burning-plasma state.[9] Once silicon dopants were added to the ablators, this trend continued further, and the first implosions with $\chi_{\mathrm{MJ}} > 0.8$ were recorded in 2022.[24] Recently, several shots have reached the scaled burning-plasma state, achieving a record $\chi_{\mathrm{MJ}} = 0.89 \pm 0.05$ and an extrapolated fusion yield of 1.5 ± 0.6 MJ. Much of the improvement to recent implosions is due to a better understanding and control of mode-1 perturbations and increased areal densities through the methods discussed in Sec. IV. Interestingly, it should be noted that several of the points shown in Fig. 3 did not come directly from the Optimization Campaign, but instead came from other cryogenic implosions on longer, ten-day fill cycles. These implosions were designed to explore specific aspects of implosions and are the subject of the following section. Because these implosions reached the scaled burning-plasma state, where a small change to χ_{MJ} can lead to a large increase in

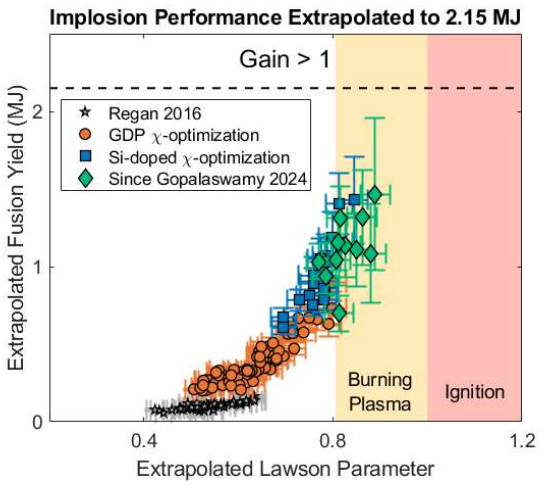

FIG. 3. The performance of the 50-Gbar campaign implosions presented in Regan *et al.*[9] (grey stars), the improvements made in part via statistical modeling in the Optimization Campaign (orange circles), the performance of Optimization implosions with silicon-doped ablators (blue squares), and the performance of cryogenic implosions since the results presented in Gopalaswamy *et al.*[24] (green diamonds), both as part of the Optimization Campaign and in other focused, high-performance experiments. The scaled burning-plasma and scaled ignition states are highlighted in yellow and red on the right, respectively, and a horizontal dashed black line indicates the extrapolated fusion yield required for a scaled gain of unity.

extrapolated yield, correcting for fuel age predicts large increases to extrapolated performance, with projected yields of up to 3.3 ± 0.8 MJ. These implosions are discussed in Sec. IV C.

IV. FOCUSED INVESTIGATIONS

Only about a third of the cryogenic experiments performed on OMEGA are part of the Optimization Campaign. The remainder are largely designed to investigate specific aspects of implosions to gain a better understanding of the underlying physics or to explore routes to increased performance. In 2023, many of these experiments focused on exploring methods to produce greater convergence and areal density. Several of these areas remain under active investigation, with new experiments and analyses planned in 2024, and their details will be published in future manuscripts once firm conclusions can be made.

A. Subcooling

Increasing the confinement of ICF implosions is necessary to achieve high-gain fusion.[27] This confinement comes by increasing the areal densities of the implosions which can be produced through greater convergence. One route to achieving greater convergence is lowering the temperature of the capsule below the DT triple point (~19 K) by a few degrees Kelvin just before the laser drive—a process known as "subcooling." Doing so reduces the amount of ice that sublimates into a vapor inside the capsule, lowering the vapor region's density. With lower initial densities, additional compression is required to counteract the drive pressure and reach stagnation.

One-dimensional simulations were performed in LILAC, reducing the DT vapor density as a function of subcooling temperature, resulting in greater convergence ratios and areal densities while roughly maintaining yields [Fig. 4(a)]. In these simulations, the areal density increased roughly proportionally to the convergence ratio. Moreover, this was achieved without adjusting the adiabat of the implosions, maintaining the stability factor, $\hat{S}$ in Eq. 3. On the other hand, as seen in that same equation, the $\hat{C}$ term indicates that the increased convergence is expected to reduce the YOC by exacerbating low- and mid-mode perturbations. Nonetheless, χ_{MJ} is more dependent on areal density than yield, and these changes are still expected to improve overall performance.

To test this hypothesis, a series of implosions were performed varying the subcooling temperature. The targets used in these implosions were standard capsules, 931 ± 5 µm in diameter with 7.5 ± 0.1-µm total wall thicknesses, the outer 5.5 µm of which was doped with Si. As shown in Fig. 4(b), the inferred areal densities increased to a point, and the yields decreased approximately as predicted. However, the improvements to areal density

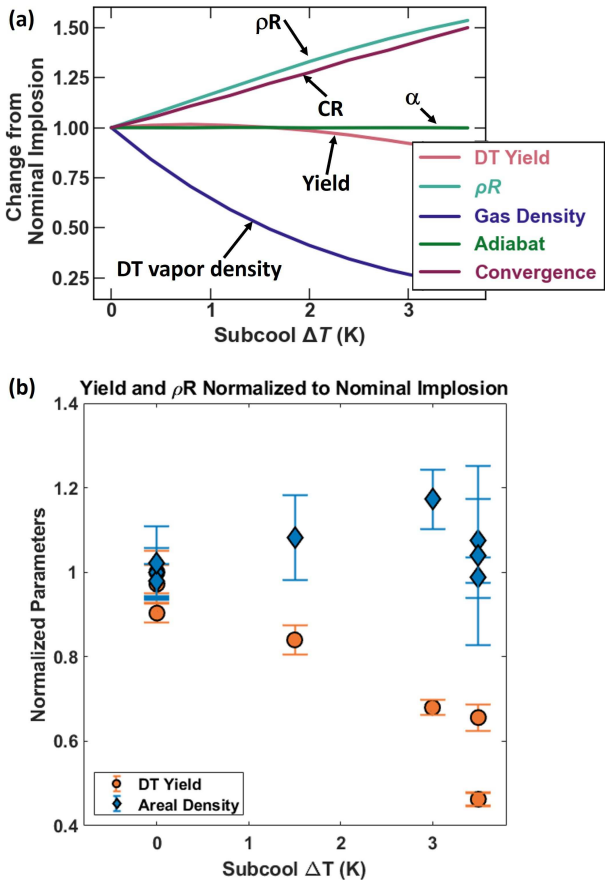

FIG. 4. (a) The results of 1D LILAC simulations are shown as the subcooling temperature is increased. These do not include any corrections from statistical modeling. (b) The experimentally measured yields and areal densities normalized to the results of nominal-temperature implosions. The data at $\Delta T = 3.5$ K suffered from significant mode-1 asymmetries, contributing to their reduced performance.

were somewhat less than LILAC predictions, resulting in only modest improvements to χ_{MJ}. This is because the inferred flow velocities were all over 100 km/s, limiting the performance of these implosions. One current hypothesis is that the increased convergence increases the growth of mode-1 perturbations, making the targets more sensitive to positioning within the chamber. Using the statistical model (Eq. 3), if these flows can be corrected in the future, subcooling at −3 K is expected to produce $\chi_{\mathrm{MJ}} \approx 0.90 \pm 0.05$. An enhanced understanding of flow measurements and offset calculations is expected to reduce these flows in upcoming experiments.

B. SSD Scan

A second route to greater convergence and performance is lowering the adiabat of the implosions. Doing so increases the shell density during the acceleration phase, reducing the thickness of the shell and enabling greater

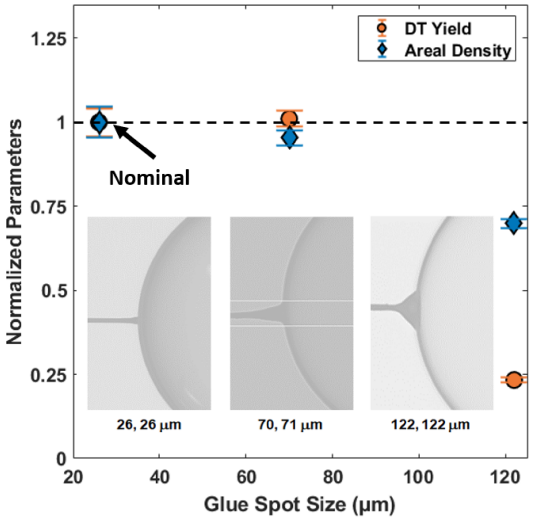

FIG. 5. Glue spot scan. The DT yields (orange circles) and areal densities (blue diamonds) are plotted against the varied cross-sectional diameters of the glue spots. Insets show shadowgraphs of the glue spots where the capsules were attached to the stalks.

compression. As discussed in Sec. II B, this also decreases the stability factor $\hat{S}$ and is expected to reduce the YOC as short-wavelength features grow to detrimental levels. Low adiabats are therefore expected to be more sensitive to laser imprint.

To test the implosions' sensitivity to imprint at different adiabats, a series of experiments were performed imploding 8-μm-thick, 980-μm-diam CD shells filled with 42 μm of DT ice.[53] These capsules were imploded with 28.5 kJ of UV energy in two pulse shapes: one setting an expected adiabat of 3.5 and the other an adiabat of 5.0. The smoothing-by-spectral-dispersion (SSD) bandwidth fraction was progressively reduced between implosions with each pulse shape. This reduced the smoothing of laser speckle, with the illumination nonuniformity going as $\sigma_{\rm rms} \simeq 20.3(\%)/\sqrt{47.5 \times \text{SSD_fraction} + 1}$, increasing the relative imprint levels.[53]

The yield and areal density measurements, normalized to the full-SSD-bandwidth measurements for each pulse shape, are plotted in Figs. 3 and 4 of Ref.[53] for both adiabats as a function of SSD bandwidth fraction. High-adiabat implosions were robust to SSD fraction with both yield and areal density degrading only when the bandwidth fraction fell below 50%. Low-adiabat implosions, on the other hand, saw immediate degradation as the SSD bandwidth fraction was lowered. This indicates that additional imprint mitigation is required before moving to these lower-adiabat, higher-performance implosion designs.[54–56]

C. Mounting Features

While the statistical model captures many design parameters, it is blind to systematic errors from sources such as mounting hardware. It is therefore important to examine the impact of these features on implosion performance.

To this end, two experimental campaigns are underway to determine the effects of mounting hardware. Capsules on OMEGA are inserted into the target chamber by gluing the targets to thin stalks that are then held by the Target Positioning System. These two campaigns vary both the size of the glue spot attaching the capsule to the stalk and the diameter of the stalk itself.

The first campaign varied the size of the glue spot from the nominal 26-μm diameter to 70 μm and 122 μm. The rest of the implosion design was kept constant, using 940-μm-OD targets with 1.9 μm of CD inner- and 5.5 μm CH-Si(6%) outer-layer ablators with 42 μm of DT ice. These targets were driven with 28.1 ± 0.2 kJ of laser energy with a standard double-spike pulse shape (SD1505Sv003 as used on top-performing shot 104949). The yield and areal densities were measured and inferred for each shot and normalized by the nominal case. As shown in Fig. 5(a), the 70-μm glue spots had nearly identical performance as the nominal implosion. Increasing further to 122 μm showed strong degradation in both performance metrics. However, it was suspected that the ice-layer quality was poor on this latter implosion, which could explain this drop in performance. Nonetheless, the nearly identical performance between the nominal 26-μm glue spot and the 70-μm glue spot suggests that the glue spot is not a significant limiting factor in these implosions.

The second campaign, varying the stalk diameter, is ongoing, and preliminary results are not yet conclusive. The target and pulse parameters were identical to the glue-spot scan, and the stalk diameter was reduced on three implosions from the nominal 14-μm diameter to 10 μm. Large flow velocities (148 ± 12 km/s) were observed during the reference implosion using a 14 μm stalk upon stagnation. In general, flows in excess of 100 km/s have been shown to limit implosion performance, relating to the $\hat{T}$ term in Eq. 3, which makes direct comparisons to small-stalk implosions in this campaign so far unreliable. However, one of the 10-μm implosions, shot 109675, produced a record $\chi_{\rm MJ} = 0.89 \pm 0.05$, exceeding the previous record of $\chi_{\rm MJ} = 0.85 \pm 0.05$ primarily through an increased areal density of 177 ± 15 g/cm^2. Additionally, this was on a long, 11-day fill cycle, whereas shot 104949 benefited from a short, four-day fill cycle. Using the statistical model to correct for fuel age increases the $\chi_{\rm MJ}$ still further to approximately 0.92 and extrapolated fusion gain above unity. Therefore, while the comparison to other shots in this campaign is not conclusive, preliminary data do align with the hypothesis that reducing the stalk diameter will improve overall performance. However, this was an extremely symmetric implosion with low flow velocities, and its symmetry could also have been

the cause of the improved performance. The fact that such high performance was achieved under nonideal conditions supports continuing the investigation into 10-µm stalks further to determine if the stalk or the implosion symmetry had the greatest effect.

D. Subscale Implosions

In the absence of laser–plasma instabilities (LPIs), it is desirable to drive ICF capsules at greater intensities. Greater intensities produce greater ablation pressures, and because the capsule has maximum surface area early in time, increasing the intensity at the beginning of the drive increases the acceleration and implosion velocity of the shell. However, the intensity is limited both by LPI, which can lead to hot-electron preheat, and by the maximum power achievable with OMEGA's laser amplifiers. As discussed in Sec. III, silicon dopants reduce LPI, increasing the intensity threshold for preheat to occur and overcoming the first challenge to fielding greater intensities. For the latter challenge, to increase the beam intensity when power is limited, the diameter of the targets must be reduced so that power is deposited over a smaller area. To maintain the R_b/R_t ratio and effectively couple the laser energy to the smaller capsules, new phase plates were developed, producing spots with diameters of approximately 650 µm instead of the full-scale 850 µm typically fielded. Experiments using the combination of smaller targets with smaller phase plates are referred to as "subscale."

A series of subscale experiments was performed with increased intensity to assess their potential for increased implosion quality and fusion performance. Capsules ∼770 µm in diameter with 6.0- to 7.0-µm-thick Si-doped ablators were filled with ∼36 µm of DT ice. These were driven with pulse shapes based on a hydrodynamic scaling of a previous full-scale implosion (Fig. 6) but with up to ∼50% increased intensity on the drive and ∼23 kJ of UV energy. The data for these implosions are still being analyzed, but preliminary analysis suggests that, with little to no optimization, these experiments met or exceeded prior hydroscaled performance achieved with larger-scale implosions. Further details will be provided in a future publication, but the results have motivated further investigations of these high-intensity experiments.

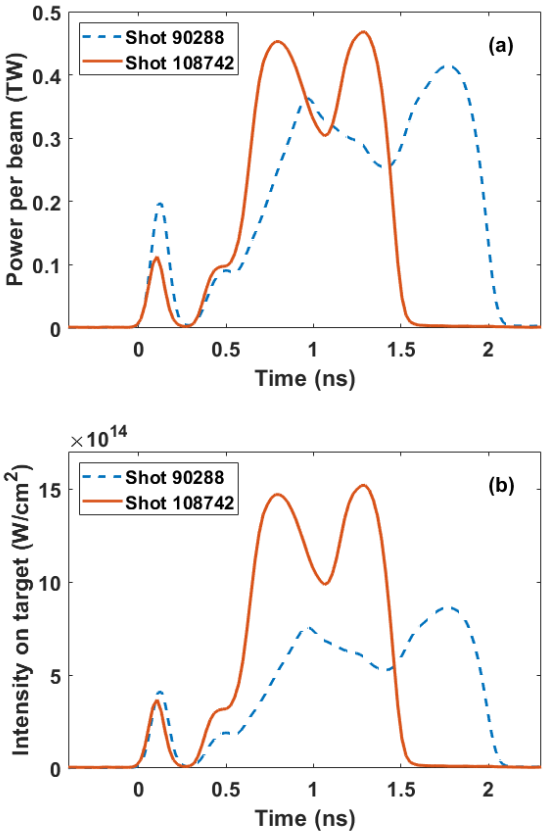

FIG. 6. Selected temporal profiles of the pulse shapes used in a subscale implosion with 22.7 kJ of drive energy (shot 108742, solid orange curve) and its lower-intensity, full-scale counterpart with 28.5 kJ of energy (shot 90288, dashed blue curve). (a) The power per beam, showing similar maximum power between the two implosions, and (b) the average intensity over the targets' initial outer surfaces, resulting from a smaller beam and target diameters in subscale.

V. FUTURE STUDIES

In the near term, several experiments are planned to continue pursuing increased convergence and areal densities in cryogenic, direct-drive ICF implosions. These include continuing efforts in the subscale, 10-µm-diam stalk, and subcooling platforms, as well as more-novel designs such as shock-augmented ignition.[57] In the medium to long term, though, perhaps the greatest limiting factor of current implosions on OMEGA is the adiabat. As stated in Sec. IV B, the minimum adiabat in a high-performance OMEGA implosion is currently around 5. Going below this level sees a rapid decrease in performance due to laser imprint as the stability factor $\hat{S}$ is decreased. Thus, new methods to mitigate the effects of laser imprint and improve $\hat{S}$ are necessary to reduce the adiabat and see significant performance improvement. To do so, innovations in target development and laser technology are required.

1. Foam Overcoats

One method to mitigate laser imprint is to coat the exterior of a capsule with a moderate 40 to 80-mg/cm^3 foam. By doing so, the density at the ablation front is reduced, resulting in greater ablation velocities and den-

sity scale lengths, both of which suppress the Rayleigh–Taylor instability.[55,58] This is the instability that amplifies laser imprint, so by limiting its growth, the effects of laser imprint are lessened. This scheme has been proven numerically to significantly improve the robustness of shells in flight.[55] The challenge is target fabrication. The foam must be produced in such a way that it does not seed its own modulations either due to large filament sizes or low-mode perturbations from large-wavelength nonuniformities. To address this challenge, a two-photon-polymerization (2PP) printing process is under development to enable the creation of designed foams with filaments down to 120 to 200 nm in diameter. Continuing to develop these capabilities is a key component of future target-based solutions to implosion stability. As these capabilities grow, experiments are planned to test the material properties of the resulting foams, the effects of foam microstructure on areal-density perturbation growth, and their robustness against experimental operations such as the fill process.

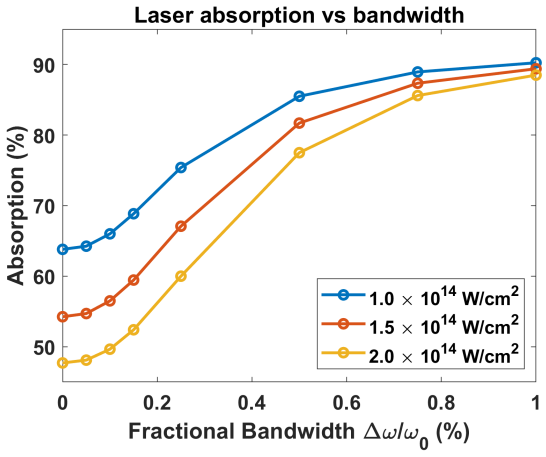

FIG. 7. Bandwidth effects on energy coupling. Shown are the calculated absorption fractions for various single-beam intensities on target as a function of driver bandwidth.

2. Hybrid Targets

In addition to lessening the growth of modulations, laser imprint itself can be reduced through target design by taking inspiration from indirect drive. As stated in the introduction, by using x rays to implode the target, indirect drive avoids the complications of laser imprint, but this comes at the cost of efficiency. This is because the incoherence of the x rays produces even illumination, driving a smooth shock into the target. However, this smoothness is only required at early times. A few hundred picoseconds after the initial shock, a conduction zone forms that exponentially reduces pressure perturbations at the ablation front, drastically reducing laser imprint.[12] Hybrid direct-drive targets combine indirect and direct drive by creating the first shock using x rays produced as a picket hits a thin, high-Z-coated membrane. After the conduction zone forms and the membrane has dissipated away, beams are then able to directly drive the preconditioned target surface.

This scheme has shown to be effective in planar experiments on OMEGA EP.[56] Work is now underway to bring these targets to a spherical geometry, where the challenge is supporting the high-Z membrane around the internal capsule. Current designs are investigating the use of low-density ($\sim$5 mg/cm^3) foams to support the membrane, as well as externally mounted curved membranes to be driven in polar-direct-drive geometries.

3. Wetted Foam

Finally, one method to improve the overall stability of implosions is to reduce the IFAR. This requires producing thicker shells in flight, which typically requires poor compression. The wetted foam concept seeks to improve upon this by replacing the inner ice layer of a cryogenic capsule with a low-density foam that is wetted with liquid DT.[59] Because this layer has a lower density than DT ice, it must be thicker to maintain the same amount of fuel, thereby resulting in a reduced IFAR. Additionally, because the liquid state of DT spans a relatively large temperature range, this also gives greater control over the vapor density of the capsule interior to allow convergence to be adjusted as needed. The same 2PP printing technology as discussed in Sec. V 1 can be used to produce foams on the inside of the capsules. In addition to continuing to refine the 2PP printing process, this design will be advanced by designing new experimental systems to wet the foams.

A. Laser Development

In addition to target designs, new laser technology is expected to significantly reduce laser imprint and LPI via broadband laser illumination. By broadening the spectrum of the laser illumination so that $\Delta\omega/\omega > 1\%$, where ω is the photon frequency, the resonant drive of LPI is disrupted. This has been shown theoretically and numerically to increase the intensity threshold for hot-electron generation by a factor of 3[60] while mitigating CBET,[61] significantly increasing the energy coupling of the laser to target up to 90% (Fig. 7).[62] To validate this bandwidth modeling, the fourth-generation laser for ultra-broadband experiments (FLUX)[63,64] is under construction. When complete, it will produce $\Delta\omega/\omega > 1\%$ with a central wavelength around 351 nm, allowing experiments to be performed to directly measure these expected benefits of bandwidth. The outcomes of broadband experiments on this system will provide a step change to implosion performance and will be central to the design of future implosion facilities.

VI. CONCLUSIONS

In the past few years, implosions on OMEGA have improved significantly. DT yields in excess of 10^{14} are now regularly achieved with extrapolated fusion yields increasing over an order of magnitude from the 50-Gbar campaign in 2016.[9] The scaled burning-plasma state has now repeatedly been achieved in cryogenic implosions with a maximum $\chi_{\mathrm{MJ}} = 0.89 \pm 0.05$ and extrapolated fusion yields of 1.5 ± 0.6 MJ when scaled to 2.15 MJ of driver energy. These studies now seek to improve the convergence of implosions to maximize areal densities and χ_{MJ}. While scans varying the SSD smoothing indicate that this is not easily achieved by lowering the adiabat of the implosions due to laser imprint, other techniques such as rapid subcooling are being explored to lower the vapor density and maximize convergence. Using smaller laser focal spots with new phase plates and proportionally smaller targets, the intensities delivered on target can be increased to improve overall performance. These routes will continue to be explored and expanded upon in the Optimization Campaign and accompanying focused studies in the near term alongside advanced target designs, such as wetted foams, foam overcoats, and hybrid-drive targets. These target innovations will be critical in the OMEGA cryogenic implosion program to mitigate laser imprint with current laser technology. This is crucial to field lower-adiabat designs and significantly improve the confinement, compression, and areal densities of implosions. In parallel, research continues into the effects of increased laser bandwidth and its expected mitigation of laser–plasma instabilities and increased energy coupling. Combined with theoretical and numerical developments and the predictive capabilities of statistical modeling, rapid progress is expected to soon reach scaled gain and ignition on the OMEGA laser. Once achieved, these results will be used to design a future direct-drive facility capable of achieving high-gain thermonuclear burn in the laboratory.

VII. ACKNOWLEDGEMENTS AND DISCLAIMERS

This material is based upon work supported by the Department of Energy [National Nuclear Security Administration] University of Rochester "National Inertial Confinement Fusion Program" under Award Number(s) DE-NA0004144. It is also funded by the DOE Office of FES under award DE-SC0022132, the National Nuclear Security Administration under Award Number DE-NA0003868. Funding for the targets utilized in this study were provided by General Atomics and funded through the NNSA contract 89233119CNA000063. This report was prepared as an account of work sponsored by an agency of the United States Government. Neither the United States Government nor any agency thereof, nor any of their employees, makes any warranty, express or implied, or assumes any legal liability or responsibility for the accuracy, completeness, or usefulness of any information, apparatus, product, or process disclosed, or represents that its use would not infringe privately owned rights. Reference herein to any specific commercial product, process, or service by trade name, trademark, manufacturer, or otherwise does not necessarily constitute or imply its endorsement, recommendation, or favoring by the United States Government or any agency thereof. The views and opinions of authors expressed herein do not necessarily state or reflect those of the United States Government or any agency thereof.

[1] J. Nuckolls, L. Wood, A. Thiessen, and G. Zimmerman, "Laser compression of matter to super-high densities: Thermonuclear (ctr) applications pressure: Implosion, ablation," (1972).

[2] S. Atzeni and J. M. ter Vehn, *The Physics of Inertial Fusion* (Oxford University Press, 2004).

[3] S. A. Slutz, M. C. Herrmann, R. A. Vesey, A. B. Sefkow, D. B. Sinars, D. C. Rovang, K. J. Peterson, and M. E. Cuneo, "Pulsed-power-driven cylindrical liner implosions of laser preheated fuel magnetized with an axial field," Physics of Plasmas **17** (2010), 10.1063/1.3333505.

[4] R. Betti, A. R. Christopherson, B. K. Spears, R. Nora, A. Bose, J. Howard, K. M. Woo, M. J. Edwards, and J. Sanz, "Alpha heating and burning plasmas in inertial confinement fusion," Physical Review Letters **114** (2015), 10.1103/PhysRevLett.114.255003.

[5] O. A. Hurricane, D. A. Callahan, D. T. Casey, E. L. Dewald, T. R. Dittrich, T. Döppner, S. Haan, D. E. Hinkel, L. F. B. Hopkins, O. Jones, A. L. Kritcher, S. L. Pape, T. Ma, A. G. Macphee, J. L. Milovich, J. Moody, A. Pak, H. S. Park, P. K. Patel, J. E. Ralph, H. F. Robey, J. S. Ross, J. D. Salmonson, B. K. Spears, P. T. Springer, R. Tommasini, F. Albert, L. R. Benedetti, R. Bionta, E. Bond, D. K. Bradley, J. Caggiano, P. M. Celliers, C. Cerjan, J. A. Church, R. Dylla-Spears, D. Edgell, M. J. Edwards, D. Fittinghoff, M. A. B. Garcia, A. Hamza, R. Hatarik, H. Herrmann, M. Hohenberger, D. Hoover, J. L. Kline, G. Kyrala, B. Kozioziemski, G. Grim, J. E. Field, J. Frenje, N. Izumi, M. G. Johnson, S. F. Khan, J. Knauer, T. Kohut, O. Landen, F. Merrill, P. Michel, A. Moore, S. R. Nagel, A. Nikroo, T. Parham, R. R. Rygg, D. Sayre, M. Schneider, D. Shaughnessy, D. Strozzi, R. P. Town, D. Turnbull, P. Volegov, A. Wan, K. Widmann, C. Wilde, and C. Yeamans, "Inertially confined fusion plasmas dominated by alpha-particle self-heating," Nature Physics **12**, 800–806 (2016).

[6] A. R. Christopherson, R. Betti, A. Bose, J. Howard, K. M. Woo, E. M. Campbell, J. Sanz, and B. K. Spears, "A comprehensive alpha-heating model for inertial confinement fusion," Physics of Plasmas **25** (2018), 10.1063/1.4991405.

[7] J. D. Lindl, P. Amendt, R. L. Berger, S. G. Glendinning, S. H. Glenzer, S. W. Haan, R. L. Kauffman, O. L. Landen, and L. J. Suter, "The physics basis for ignition using indirect-drive targets on the national ignition facility," Physics of Plasmas **11**, 339–491 (2004).

[8] R. Betti, K. Anderson, V. N. Goncharov, R. L. McCrory, D. D. Meyerhofer, S. Skupsky, and R. P. Town, "Deceleration phase of inertial confinement fusion implosions," Physics of Plasmas **9**, 2277–2286 (2002).

[9] S. P. Regan, V. N. Goncharov, I. V. Igumenshchev, T. C. Sangster, R. Betti, A. Bose, T. R. Boehly, M. J. Bonino, E. M. Campbell, D. Cao, T. J. Collins, R. S. Craxton, A. K. Davis, J. A. Delettrez, D. H. Edgell, R. Epstein, C. J. Forrest, J. A. Frenje, D. H. Froula, M. G. Johnson, V. Y. Glebov, D. R. Harding, M. Hohenberger, S. X. Hu, D. Jacobs-Perkins, R. Janezic, M. Karasik, R. L. Keck, J. H. Kelly, T. J. Kessler, J. P. Knauer, T. Z. Kosc, S. J. Loucks, J. A. Marozas, F. J. Marshall, R. L. McCrory, P. W. McKenty, D. D. Meyerhofer, D. T. Michel, J. F. Myatt, S. P. Obenschain, R. D. Petrasso, P. B. Radha, B. Rice, M. J. Rosenberg, A. J. Schmitt, M. J. Schmitt, W. Seka, W. T.

Shmayda, M. J. Shoup, A. Shvydky, S. Skupsky, A. A. Solodov, C. Stoeckl, W. Theobald, J. Ulreich, M. D. Wittman, K. M. Woo, B. Yaakobi, and J. D. Zuegel, "Demonstration of fuel hot-spot pressure in excess of 50 gbar for direct-drive, layered deuterium-tritium implosions on omega," Physical Review Letters **117** (2016), 10.1103/PhysRevLett.117.025001.

[10] A. L. Kritcher, C. V. Young, H. F. Robey, C. R. Weber, A. B. Zylstra, O. A. Hurricane, D. A. Callahan, J. E. Ralph, J. S. Ross, K. L. Baker, D. T. Casey, D. S. Clark, T. Döppner, L. Divol, M. Hohenberger, L. B. Hopkins, S. L. Pape, N. B. Meezan, A. Pak, P. K. Patel, R. Tommasini, S. J. Ali, P. A. Amendt, L. J. Atherton, B. Bachmann, D. Bailey, L. R. Benedetti, R. Betti, S. D. Bhandarkar, J. Biener, R. M. Bionta, N. W. Birge, E. J. Bond, D. K. Bradley, T. Braun, T. M. Briggs, M. W. Bruhn, P. M. Celliers, B. Chang, T. Chapman, H. Chen, C. Choate, A. R. Christopherson, J. W. Crippen, E. L. Dewald, T. R. Dittrich, M. J. Edwards, W. A. Farmer, J. E. Field, D. Fittinghoff, J. A. Frenje, J. A. Gaffney, M. G. Johnson, S. H. Glenzer, G. P. Grim, S. Haan, K. D. Hahn, G. N. Hall, B. A. Hammel, J. Harte, E. Hartouni, J. E. Heebner, V. J. Hernandez, H. Herrmann, M. C. Herrmann, D. E. Hinkel, D. D. Ho, J. P. Holder, W. W. Hsing, H. Huang, K. D. Humbird, N. Izumi, L. C. Jarrott, J. Jeet, O. Jones, G. D. Kerbel, S. M. Kerr, S. F. Khan, J. Kilkenny, Y. Kim, H. Geppert-Kleinrath, V. Geppert-Kleinrath, C. Kong, J. M. Koning, M. K. Kruse, J. J. Kroll, B. Kustowski, O. L. Landen, S. Langer, D. Larson, N. C. Lemos, J. D. Lindl, T. Ma, M. J. MacDonald, B. J. MacGowan, A. J. Mackinnon, S. A. MacLaren, A. G. MacPhee, M. M. Marinak, D. A. Mariscal, E. V. Marley, L. Masse, K. Meaney, P. A. Michel, M. Millot, J. L. Milovich, J. D. Moody, A. S. Moore, J. W. Morton, T. Murphy, K. Newman, J. M. D. Nicola, A. Nikroo, R. Nora, M. V. Patel, L. J. Pelz, J. L. Peterson, Y. Ping, B. B. Pollock, M. Ratledge, N. G. Rice, H. Rinderknecht, M. Rosen, M. S. Rubery, J. D. Salmonson, J. Sater, S. Schiaffino, D. J. Schlossberg, M. B. Schneider, C. R. Schroeder, H. A. Scott, S. M. Sepke, K. Sequoia, M. W. Sherlock, S. Shin, V. A. Smalyuk, B. K. Spears, P. T. Springer, M. Stadermann, S. Stoupin, D. J. Strozzi, L. J. Suter, C. A. Thomas, R. P. Town, C. Trosseille, E. R. Tubman, P. L. Volegov, K. Widmann, C. Wild, C. H. Wilde, B. M. V. Wonterghem, D. T. Woods, B. N. Woodworth, M. Yamaguchi, S. T. Yang, and G. B. Zimmerman, "Design of inertial fusion implosions reaching the burning plasma regime," Nature Physics **18**, 251–258 (2022).

[11] P. B. Radha, M. Hohenberger, D. H. Edgell, J. A. Marozas, F. J. Marshall, D. T. Michel, M. J. Rosenberg, W. Seka, A. Shvydky, T. R. Boehly, T. J. B. Collins, E. M. Campbell, R. S. Craxton, J. A. Delettrez, S. N. Dixit, J. A. Frenje, D. H. Froula, V. N. Goncharov, S. X. Hu, J. P. Knauer, R. L. McCrory, P. W. McKenty, D. D. Meyerhofer, J. Moody, J. F. Myatt, R. D. Petrasso, S. P. Regan, T. C. Sangster, H. Sio, S. Skupsky, and A. Zylstra, "Direct drive: Simulations and results from the national ignition facility," Physics of Plasmas **23**, 056305 (2016).

[12] R. S. Craxton, K. S. Anderson, T. R. Boehly, V. N. Goncharov, D. R. Harding, J. P. Knauer, R. L. McCrory, P. W. McKenty, D. D. Meyerhofer, J. F. Myatt, A. J. Schmitt, J. D. Sethian, R. W. Short, S. Skupsky, W. Theobald, W. L. Kruer, K. A. Tanaka, R. Betti, T. J. B. Collins, J. A. Delettrez, S. X. Hu, J. A. Marozas, A. V. Maximov, D. T. Michel, P. B. Radha, S. P. Regan, T. C. Sangster, W. Seka, A. A. Solodov, J. M. Soures, C. Stoeckl, and J. D. Zuegel, "Direct-drive inertial confinement fusion: A review," Physics of Plasmas **22**, 110501 (2015).

[13] T. R. Boehly, A. Babushkin, D. K. Bradley, R. S. Craxton, J. A. Delettrez, R. Epstein, T. J. Kessler, J. P. Knauer, R. L. McCrory, P. W. McKenty, D. D. Meyerhofer, S. Regan, W. Seka, S. Skupsky, V. A. Smalyuk, R. P. Town, and B. Yaakobi, "Laser uniformity and hydrodynamic stability experiments at the omega laser facility," Laser and Particle Beams **18**, 11–19 (2000).

[14] P. B. Radha, V. N. Goncharov, T. J. B. Collins, J. A. Delettrez, Y. Elbaz, V. Y. Glebov, R. L. Keck, D. E. Keller, J. P. Knauer, J. A. Marozas, F. J. Marshall, P. W. McKenty, D. D. Meyerhofer, S. P. Regan, T. C. Sangster, D. Shvarts, S. Skupsky, Y. Srebro, R. P. J. Town, and C. Stoeckl, "Two-dimensional simulations of plastic-shell, direct-drive implosions on omega," Physics of Plasmas **12**, 032702 (2005).

[15] I. V. Igumenshchev, D. T. Michel, R. C. Shah, E. M. Campbell, R. Epstein, C. J. Forrest, V. Y. Glebov, V. N. Goncharov, J. P. Knauer, F. J. Marshall, R. L. McCrory, S. P. Regan, T. C. Sangster, C. Stoeckl, A. J. Schmitt, and S. Obenschain, "Three-dimensional hydrodynamic simulations of omega implosions," Physics of Plasmas **24** (2017), 10.1063/1.4979195.

[16] V. A. Smalyuk, V. N. Goncharov, K. S. Anderson, R. Betti, R. S. Craxton, J. A. Delettrez, D. D. Meyerhofer, S. P. Regan, and T. C. Bangster, "Measurements of the effects of the intensity pickets on laser imprinting for direct-drive, adiabat-shaping designs on omega," Physics of Plasmas **14** (2007), 10.1063/1.2715550.

[17] S. X. Hu, D. T. Michel, A. K. Davis, R. Betti, P. B. Radha, E. M. Campbell, D. H. Froula, and C. Stoeckl, "Understanding the effects of laser imprint on plastic-target implosions on omega," Physics of Plasmas **23**, 102701 (2016).

[18] J. L. Peebles, S. X. Hu, W. Theobald, V. N. Goncharov, N. Whiting, P. M. Celliers, S. J. Ali, G. Duchateau, E. M. Campbell, T. R. Boehly, and S. P. Regan, "Direct-drive measurements of laser-imprint-induced shock velocity nonuniformities," Physical Review E **99** (2019), 10.1103/PhysRevE.99.063208.

[19] A. B. Zylstra, A. L. Kritcher, O. A. Hurricane, D. A. Callahan, J. E. Ralph, D. T. Casey, A. Pak, O. L. Landen, B. Bachmann, K. L. Baker, L. B. Hopkins, S. D. Bhandarkar, J. Biener, R. M. Bionta, N. W. Birge, T. Braun, T. M. Briggs, P. M. Celliers, H. Chen, C. Choate, D. S. Clark, L. Divol, T. Döppner, D. Fittinghoff, M. J. Edwards, M. G. Johnson, N. Gharibyan, S. Haan, K. D. Hahn, E. Hartouni, D. E. Hinkel, D. D. Ho, M. Hohenberger, J. P. Holder, H. Huang, N. Izumi, J. Jeet, O. Jones, S. M. Kerr, S. F. Khan, H. G. Kleinrath, V. G. Kleinrath, C. Kong, K. M. Lamb, S. L. Pape, N. C. Lemos, J. D. Lindl, B. J. Macgowan, A. J. Mackinnon, A. G. Macphee, E. V. Marley, K. Meaney, M. Millot, A. S. Moore, K. Newman, J. M. D. Nicola, A. Nikroo, R. Nora, P. K. Patel, N. G. Rice, M. S. Rubery, J. Sater, D. J. Schlossberg, S. M. Sepke, K. Sequoia, S. J. Shin, M. Stadermann, S. Stoupin, D. J. Strozzi, C. A. Thomas, R. Tommasini, C. Trosseille, E. R. Tubman, P. L. Volegov, C. R. Weber, C. Wild, D. T. Woods, S. T. Yang, and C. V. Young, "Experimental achievement and signatures of ignition at the national ignition facility," Physical Review E **106** (2022), 10.1103/PhysRevE.106.025202.

[20] H. Abu-Shawareb, R. Acree, P. Adams, J. Adams, *et al.*, "Lawson criterion for ignition exceeded in an inertial fusion experiment," Physical Review Letters **129** (2022), 10.1103/PhysRevLett.129.075001.

[21] O. A. Hurricane, D. A. Callahan, D. T. Casey, A. R. Christopherson, A. L. Kritcher, O. L. Landen, S. A. Maclaren, R. Nora, P. K. Patel, J. Ralph, D. Schlossberg, P. T. Springer, C. V. Young, and A. B. Zylstra, "Energy principles of scientific breakeven in an inertial fusion experiment," Physical Review Letters **132** (2024), 10.1103/PhysRevLett.132.065103.

[22] E. I. Moses, "The national ignition facility (nif): A path to fusion energy," Energy Conversion and Management **49**, 1795–1802 (2008).

[23] T. R. Boehly, D. L. Brown, R. S. Craxton, R. L. Keck, J. P. Knauer, J. H. Kelly, T. J. Kessler, S. A. Kumpan, S. J. Bucks, S. A. Letzring, F. J. Marshall, R. L. Mccrory, S. F. B. Morse, W. Seka, J. M. Sow-Es, and C. P. Verdon, "Initial performance results of the omega laser system," Optics Communications **133**, 495–506 (1997).

[24] V. Gopalaswamy, C. A. Williams, R. Betti, D. Patel, J. P. Knauer, A. Lees, D. Cao, E. M. Campbell, P. Farmakis, R. Ejaz, K. S. Anderson, R. Epstein, J. Carroll-Nellenbeck, I. V. Igumenshchev, J. A. Marozas, P. B. Radha, A. A. Solodov, C. A. Thomas, K. M. Woo, T. J. Collins, S. X. Hu, W. Scullin, D. Turnbull, V. N. Goncharov, K. Churnetski, C. J. Forrest, V. Y. Glebov, P. V. Heuer, H. McClow, R. C. Shah, C. Stoeckl,

W. Theobald, D. H. Edgell, S. Ivancic, M. J. Rosenberg, S. P. Regan, D. Bredesen, C. Fella, M. Koch, R. T. Janezic, M. J. Bonino, D. R. Harding, K. A. Bauer, S. Sampat, L. J. Waxer, M. Labuzeta, S. F. Morse, M. Gatu-Johnson, R. D. Petrasso, J. A. Frenje, J. Murray, B. Serrato, D. Guzman, C. Shuldberg, M. Farrell, and C. Deeney, "Demonstration of a hydrodynamically equivalent burning plasma in direct-drive inertial confinement fusion," Nature Physics (2024), 10.1038/s41567-023-02361-4.

[25]V. Gopalaswamy, R. Betti, J. P. Knauer, N. Luciani, D. Patel, K. M. Woo, A. Bose, I. V. Igumenshchev, E. M. Campbell, K. S. Anderson, K. A. Bauer, M. J. Bonino, D. Cao, A. R. Christopherson, G. W. Collins, T. J. B. Collins, J. R. Davies, J. A. Delettrez, D. H. Edgell, R. Epstein, C. J. Forrest, D. H. Froula, V. Y. Glebov, V. N. Goncharov, D. R. Harding, S. X. Hu, D. W. Jacobs-Perkins, R. T. Janezic, J. H. Kelly, O. M. Mannion, A. Maximov, F. J. Marshall, D. T. Michel, S. Miller, S. F. B. Morse, J. Palastro, J. Peebles, P. B. Radha, S. P. Regan, S. Sampat, T. C. Sangster, A. B. Sefkow, W. Seka, R. C. Shah, W. T. Shmyada, A. Shvydky, C. Stoeckl, A. A. Solodov, W. Theobald, J. D. Zuegel, M. G. Johnson, R. D. Petrasso, C. K. Li, and J. A. Frenje, "Tripled yield in direct-drive laser fusion through statistical modelling," Nature **565**, 581–586 (2019).

[26]M. J. Rosenberg, A. A. Solodov, C. Stoeckl, M. Hohenberger, R. Bahukutumbi, W. Theobald, D. Edgell, T. Filkins, R. Betti, F. J. Marshall, R. C. Shah, D. P. Turnbull, A. R. Christopherson, N. Lemos, E. Tubman, and S. P. Regan, "Hot electron preheat in hydrodynamically scaled direct-drive inertial confinement fusion implosions on the nif and omega," Physics of Plasmas **30**, 072710 (2023).

[27]J. D. Lawson, "Some criteria for a power producing thermonuclear reactor," Proceedings of the Physical Society. Section B **70**, 6–10 (1957).

[28]R. Betti, P. Y. Chang, B. K. Spears, K. S. Anderson, J. Edwards, M. Fatenejad, J. D. Lindl, R. L. McCrory, R. Nora, and D. Shvarts, "Thermonuclear ignition in inertial confinement fusion and comparison with magnetic confinement," Physics of Plasmas **17**, 058102 (2010).

[29]P. Chang, R. Betti, B. K. Spears, K. S. Anderson, J. Edwards, M. Fatenejad, J. D. Lindl, R. L. McCrory, R. Nora, and D. Shvarts, "Generalized measurable ignition criterion for inertial confinement fusion," Physical Review Letters **104** (2010), 10.1103/PhysRevLett.104.135002.

[30]A. Bose, K. M. Woo, R. Betti, E. M. Campbell, D. Mangino, A. R. Christopherson, R. L. McCrory, R. Nora, S. P. Regan, V. N. Goncharov, T. C. Sangster, C. J. Forrest, J. Frenje, M. G. Johnson, V. Y. Glebov, J. P. Knauer, F. J. Marshall, C. Stoeckl, and W. Theobald, "Core conditions for alpha heating attained in direct-drive inertial confinement fusion," Physical Review E **94** (2016), 10.1103/PhysRevE.94.011201.

[31]R. Nora, R. Betti, K. S. Anderson, A. Shvydky, A. Bose, K. M. Woo, A. R. Christopherson, J. A. Marozas, T. J. Collins, P. B. Radha, S. X. Hu, R. Epstein, F. J. Marshall, R. L. McCrory, T. C. Sangster, and D. D. Meyerhofer, "Theory of hydro-equivalent ignition for inertial fusion and its applications to omega and the national ignition facility," Physics of Plasmas **21** (2014), 10.1063/1.4875331.

[32]A. R. Christopherson, R. Betti, C. J. Forrest, J. Howard, W. Theobald, J. A. Delettrez, M. J. Rosenberg, A. A. Solodov, C. Stoeckl, D. Patel, V. Gopalaswamy, D. Cao, J. L. Peebles, D. H. Edgell, W. Seka, R. Epstein, M. S. Wei, M. G. Johnson, R. Simpson, S. P. Regan, and E. M. Campbell, "Direct measurements of dt fuel preheat from hot electrons in direct-drive inertial confinement fusion," Physical Review Letters **127** (2021), 10.1103/PhysRevLett.127.055001.

[33]D. S. Clark, C. R. Weber, J. L. Milovich, A. E. Pak, D. T. Casey, B. A. Hammel, D. D. Ho, O. S. Jones, J. M. Koning, A. L. Kritcher, M. M. Marinak, L. P. Masse, D. H. Munro, M. V. Patel, P. K. Patel, H. F. Robey, C. R. Schroeder, S. M. Sepke, and M. J. Edwards, "Three-dimensional modeling and hydrodynamic scaling of national ignition facility implosions," Physics of Plasmas **26** (2019), 10.1063/1.5091449.

[34]D. T. Casey, C. A. Thomas, K. L. Baker, B. K. Spears, M. Hohenberger, S. F. Khan, R. C. Nora, C. R. Weber, D. T. Woods, O. A. Hurricane, D. A. Callahan, R. L. Berger, J. L. Milovich, P. K. Patel, T. Ma, A. Pak, L. R. Benedetti, M. Millot, C. Jarrott, O. L. Landen, R. M. Bionta, B. J. MacGowan, D. J. Strozzi, M. Stadermann, J. Biener, A. Nikroo, C. S. Goyon, N. Izumi, S. R. Nagel, B. Bachmann, P. L. Volegov, D. N. Fittinghoff, G. P. Grim, C. B. Yeamans, M. G. Johnson, J. A. Frenje, N. Rice, C. Kong, J. Crippen, J. Jaquez, K. Kangas, and C. Wild, "The high velocity, high adiabat, "bigfoot" campaign and tests of indirect-drive implosion scaling," Physics of Plasmas **25** (2018), 10.1063/1.5019741.

[35]S. Palaniyappan, J. P. Sauppe, B. J. Tobias, C. F. Kawaguchi, K. A. Flippo, A. B. Zylstra, O. L. Landen, D. Shvarts, E. Malka, S. H. Batha, P. A. Bradley, E. N. Loomis, N. N. Vazirani, L. Kot, D. W. Schmidt, T. H. Day, R. Gonzales, and J. L. Kline, "Hydroscaling of direct-drive cylindrical implosions at the omega and the national ignition facility," Physics of Plasmas **27** (2020), 10.1063/1.5144608.

[36]I. V. Igumenshchev, V. N. Goncharov, F. J. Marshall, J. P. Knauer, E. M. Campbell, C. J. Forrest, D. H. Froula, V. Y. Glebov, R. L. McCrory, S. P. Regan, T. C. Sangster, S. Skupsky, and C. Stoeckl, "Three-dimensional modeling of direct-drive cryogenic implosions on omega," Physics of Plasmas **23** (2016), 10.1063/1.4948418.

[37]A. Colaïtis, I. Igumenshchev, J. Mathiaud, and V. Goncharov, "Inverse ray tracing on icosahedral tetrahedron grids for non-linear laser plasma interaction coupled to 3d radiation hydrodynamics," Journal of Computational Physics **443** (2021), 10.1016/j.jcp.2021.110537.

[38]S. C. Miller and V. N. Goncharov, "Instability seeding mechanisms due to internal defects in inertial confinement fusion targets," Physics of Plasmas **29** (2022), 10.1063/5.0091949.

[39]R. K. Follett, D. H. Edgell, D. H. Froula, V. N. Goncharov, I. V. Igumenshchev, J. G. Shaw, and J. F. Myatt, "Full-wave and ray-based modeling of cross-beam energy transfer between laser beams with distributed phase plates and polarization smoothing," Physics of Plasmas **24** (2017), 10.1063/1.4998713.

[40]A. Colaïtis, D. P. Turnbull, I. V. Igumenschev, D. Edgell, R. C. Shah, O. M. Mannion, C. Stoeckl, D. Jacob-Perkins, A. Shvydky, R. Janezic, A. Kalb, D. Cao, C. J. Forrest, J. Kwiatkowski, S. Regan, W. Theobald, V. N. Goncharov, and D. H. Froula, "3d simulations capture the persistent low-mode asymmetries evident in laser-direct-drive implosions on omega," Physical Review Letters **129** (2022), 10.1103/PhysRevLett.129.095001.

[41]K. Churnetski, K. M. Woo, W. Theobald, P. B. Radha, R. Betti, V. Gopalaswamy, I. V. Igumenshchev, S. T. Ivancic, M. Michalko, R. C. Shah, C. Stoeckl, C. A. Thomas, and S. P. Regan, "Three-dimensional hot-spot x-ray emission tomography from cryogenic deuterium-tritium direct-drive implosions on omega," Review of Scientific Instruments **93** (2022), 10.1063/5.0098977.

[42]K. M. Woo, R. Betti, C. A. Thomas, C. Stoeckl, K. Churnetski, C. J. Forrest, Z. L. Mohamed, B. Zirps, S. P. Regan, T. J. Collins, W. Theobald, R. C. Shah, O. M. Mannion, D. Patel, D. Cao, J. P. Knauer, V. Y. Glebov, V. N. Goncharov, P. B. Radha, H. G. Rinderknecht, R. Epstein, V. Gopalaswamy, F. J. Marshall, S. T. Ivancic, and E. M. Campbell, "Analysis of core asymmetries in inertial confinement fusion implosions using three-dimensional hot-spot reconstruction," Physics of Plasmas **29** (2022), 10.1063/5.0102167.

[43]V. Gopalaswamy, R. Betti, J. P. Knauer, A. Lees, D. Patel, A. R. Christopherson, I. V. Igumenshchev, D. Cao, K. S. Anderson, A. Shvydky, D. H. Edgell, O. M. Mannion, C. Thomas, W. Theobald, C. Stoeckl, S. P. Regan, V. N. Goncharov, R. Shah, and E. M. Campbell, "Using statistical modeling to predict and understand fusion experiments," Physics of Plasmas **28** (2021), 10.1063/5.0056662.

[44]A. Lees, R. Betti, J. P. Knauer, V. Gopalaswamy, D. Patel, K. M. Woo, K. S. Anderson, E. M. Campbell, D. Cao,

J. Carroll-Nellenback, R. Epstein, C. J. Forrest, V. N. Goncharov, D. R. Harding, S. X. Hu, I. V. Igumenshchev, R. T. Janezic, O. M. Mannion, P. B. Radha, S. P. Regan, A. Shvydky, R. C. Shah, W. T. Shmayda, C. Stoeckl, W. Theobald, and C. A. Thomas, "Understanding the fusion yield dependencies in omega dt-layered implosion experiments using a physics-based statistical mapping model," Physics of Plasmas **30** (2023), 10.1063/5.0106515.

[45]V. N. Goncharov, T. C. Sangster, R. Betti, T. R. Boehly, M. J. Bonino, T. J. Collins, R. S. Craxton, J. A. Delettrez, D. H. Edgell, R. Epstein, R. K. Follett, C. J. Forrest, D. H. Froula, V. Y. Glebov, D. R. Harding, R. J. Henchen, S. X. Hu, I. V. Igumenshchev, R. Janezic, J. H. Kelly, T. J. Kessler, T. Z. Kosc, S. J. Loucks, J. A. Marozas, F. J. Marshall, A. V. Maximov, R. L. McCrory, P. W. McKenty, D. D. Meyerhofer, D. T. Michel, J. F. Myatt, R. Nora, P. B. Radha, S. P. Regan, W. Seka, W. T. Shmayda, R. W. Short, A. Shvydky, S. Skupsky, C. Stoeckl, B. Yaakobi, J. A. Frenje, M. Gatu-Johnson, R. D. Petrasso, and D. T. Casey, "Improving the hot-spot pressure and demonstrating ignition hydrodynamic equivalence in cryogenic deuterium-tritium implosions on omega," Physics of Plasmas **21** (2014), 10.1063/1.4876618.

[46]H. Zhang, R. Betti, R. Yan, and H. Aluie, "Nonlinear bubble competition of the multimode ablative rayleigh–taylor instability and applications to inertial confinement fusion," Physics of Plasmas **27**, 122701 (2020).

[47]T. J. Collins, C. Stoeckl, R. Epstein, W. A. Bittle, C. J. Forrest, V. Y. Glebov, V. N. Goncharov, D. R. Harding, S. X. Hu, D. W. Jacobs-Perkins, T. Z. Kosc, J. A. Marozas, C. Mileham, F. J. Marshall, S. F. Morse, P. B. Radha, S. P. Regan, B. Rice, T. C. Sangster, M. J. Shoup, W. T. Shmayda, C. Sorce, W. Theobald, and M. D. Wittman, "Causes of fuel–ablator mix inferred from modeling of monochromatic time-gated radiography of omega cryogenic implosions," Physics of Plasmas **29** (2022), 10.1063/5.0060477.

[48]K. M. Woo, R. Betti, D. Shvarts, A. Bose, D. Patel, R. Yan, P. Y. Chang, O. M. Mannion, R. Epstein, J. A. Delettrez, M. Charissis, K. S. Anderson, P. B. Radha, A. Shvydky, I. V. Igumenshchev, V. Gopalaswamy, A. R. Christopherson, J. Sanz, and H. Aluie, "Effects of residual kinetic energy on yield degradation and ion temperature asymmetries in inertial confinement fusion implosions," Physics of Plasmas **25** (2018), 10.1063/1.5026706.

[49]O. M. Mannion, I. V. Igumenshchev, K. S. Anderson, R. Betti, E. M. Campbell, D. Cao, C. J. Forrest, M. G. Johnson, V. Y. Glebov, V. N. Goncharov, V. Gopalaswamy, S. T. Ivancic, D. W. Jacobs-Perkins, A. Kalb, J. P. Knauer, J. Kwiatkowski, A. Lees, F. J. Marshall, M. Michalko, Z. L. Mohamed, D. Patel, H. G. Rinderknecht, R. C. Shah, C. Stoeckl, W. Theobald, K. M. Woo, and S. P. Regan, "Mitigation of mode-one asymmetry in laser-direct-drive inertial confinement fusion implosions," Physics of Plasmas **28** (2021), 10.1063/5.0041554.

[50]O. A. Hurricane, D. T. Casey, O. Landen, A. L. Kritcher, R. Nora, P. K. Patel, J. A. Gaffney, K. D. Humbird, J. E. Field, M. K. Kruse, J. L. Peterson, and B. K. Spears, "An analytic asymmetric-piston model for the impact of mode-1 shell asymmetry on icf implosions," Physics of Plasmas **27** (2020), 10.1063/5.0001335.

[51]F. H. Séguin, C. K. Li, J. L. DeCiantis, J. A. Frenje, J. R. Rygg, R. D. Petrasso, F. J. Marshall, V. Smalyuk, V. Y. Glebov, J. P. Knauer, T. C. Sangster, J. D. Kilkenny, and A. Nikroo, "Effects of fuel-capsule shimming and drive asymmetry on inertial-confinement-fusion symmetry and yield," Physics of Plasmas **23** (2016), 10.1063/1.4943883.

[52]C. Stoeckl, D. Cao, L. Ceurvorst, A. Kalb, J. Kwiatkowski, A. Shvydky, and W. Theobald, "Beam-pointing verification using x-ray pinhole cameras on the 60-beam omega laser," Review of Scientific Instruments **93** (2022), 10.1063/5.0098941.

[53]D. Patel, J. P. Knauer, D. Cao, R. Betti, R. Nora, A. Shvydky, V. Gopalaswamy, A. Lees, S. Sampat, W. R. Donaldson, S. P. Regan, C. Stoeckl, C. J. Forrest, V. Y. Glebov, D. R. Harding, M. J. Bonino, R. T. Janezic, D. Wasilewski, C. Fella, C. Shuldberg, J. Murray, D. Guzman, and B. Serrato, "Effects of laser bandwidth in direct-drive high-performance dt-layered implosions on the omega laser," Physical Review Letters **131** (2023), 10.1103/PhysRevLett.131.105101.

[54]S. X. Hu, G. Fiksel, V. N. Goncharov, S. Skupsky, D. D. Meyerhofer, and V. A. Smalyuk, "Mitigating laser imprint in direct-drive inertial confinement fusion implosions with high-z dopants," Physical Review Letters **108**, 195003 (2012).

[55]S. X. Hu, W. Theobald, P. B. Radha, J. L. Peebles, S. P. Regan, A. Nikroo, M. J. Bonino, D. R. Harding, V. N. Goncharov, N. Petta, T. C. Sangster, and E. M. Campbell, "Mitigating laser-imprint effects in direct-drive inertial confinement fusion implosions with an above-critical-density foam layer," Physics of Plasmas **25**, 082710 (2018).

[56]L. Ceurvorst, R. Betti, A. Casner, V. Gopalaswamy, A. Bose, S. X. Hu, E. M. Campbell, S. P. Regan, C. A. McCoy, M. Karasik, J. Peebles, M. Tabak, and W. Theobald, "Hybrid target design for imprint mitigation in direct-drive inertial confinement fusion," Physical Review E **101**, 063207 (2020).

[57]R. H. Scott, D. Barlow, W. Trickey, A. Ruocco, K. Glize, L. Antonelli, M. Khan, and N. C. Woolsey, "Shock-augmented ignition approach to laser inertial fusion," Physical Review Letters **129** (2022), 10.1103/PhysRevLett.129.195001.

[58]R. Betti, V. N. Goncharov, R. L. McCrory, and C. P. Verdon, "Growth rates of the ablative rayleigh–taylor instability in inertial confinement fusion," Physics of Plasmas **5**, 1446–1454 (1998).

[59]R. E. Olson, R. J. Leeper, J. L. Kline, A. B. Zylstra, S. A. Yi, J. Biener, T. Braun, B. J. Kozioziemski, J. D. Sater, P. A. Bradley, R. R. Peterson, B. M. Haines, L. Yin, L. F. B. Hopkins, N. B. Meezan, C. Walters, M. M. Biener, C. Kong, J. W. Crippen, G. A. Kyrala, R. C. Shah, H. W. Herrmann, D. C. Wilson, A. V. Hamza, A. Nikroo, and S. H. Batha, "First liquid layer inertial confinement fusion implosions at the national ignition facility," Physical Review Letters **117**, 245001 (2016).

[60]R. K. Follett, J. G. Shaw, J. F. Myatt, C. Dorrer, D. H. Froula, and J. P. Palastro, "Thresholds of absolute instabilities driven by a broadband laser," Physics of Plasmas **26** (2019), 10.1063/1.5098479.

[61]J. W. Bates, R. K. Follett, J. G. Shaw, S. P. Obenschain, R. H. Lehmberg, J. F. Myatt, J. L. Weaver, D. M. Kehne, M. F. Wolford, M. C. Myers, and T. J. Kessler, "Suppressing cross-beam energy transfer with broadband lasers," High Energy Density Physics **36** (2020), 10.1016/j.hedp.2020.100772.

[62]R. K. Follett, A. Colaïtis, A. G. Seaton, H. Wen, D. Turnbull, D. H. Froula, and J. P. Palastro, "Ray-based cross-beam energy transfer modeling for broadband lasers," Physics of Plasmas **30** (2023), 10.1063/5.0137420.

[63]C. Dorrer, E. M. Hill, and J. D. Zuegel, "High-energy parametric amplification of spectrally incoherent broadband pulses," Optics Express **28**, 451 (2020).

[64]C. Dorrer, M. Spilatro, S. Herman, T. Borger, and E. M. Hill, "Broadband sum-frequency generation of spectrally incoherent pulses," Optics Express **29**, 16135 (2021).